

# Association and Surface Properties of Poly(ethylene oxide)–Poly(styrene oxide) Diblock Copolymers in Aqueous Solution

Shaomin Mai,<sup>\*,†</sup> Colin Booth,<sup>†</sup> Antonis Kelarakis,<sup>‡</sup> Vasiliki Havredaki,<sup>‡</sup> and Anthony J. Ryan<sup>§</sup>

Department of Chemistry, University of Manchester, Manchester M13 9PL, U.K.,  
National and Kapodistrian University of Athens, Department of Chemistry,  
Physical Chemistry Laboratory, Panepistimiopolis, 157 71 Athens, Greece, and  
Department of Chemistry, University of Sheffield, Sheffield S3 7HF, U.K.

Received July 26, 1999. In Final Form: October 4, 1999

The association and surface properties of three oxyethylene/oxyphenylethylene (ES) diblock copolymers in aqueous solution have been studied. Copolymers E<sub>50</sub>S<sub>3.5</sub>, E<sub>50</sub>S<sub>5.1</sub>, and E<sub>51</sub>S<sub>6.5</sub> were synthesized and characterized by gel permeation chromatography and <sup>13</sup>C NMR spectroscopy. Surface tensiometry was used to determine critical micelle concentrations (cmc) at several temperatures, and thereby values of the enthalpy of micellization ( $\Delta_{\text{mic}}H^{\circ}$ ). The values of cmc and  $\Delta_{\text{mic}}H^{\circ}$  were found to be low (e.g., 0.03 g dm<sup>-3</sup> at 30 °C and 12 kJ mol<sup>-1</sup> for E<sub>51</sub>S<sub>6.5</sub>), which is consistent with the high hydrophobicity of oxyphenylethylene block. Dynamic and static light scattering were used to characterize the micelles in dilute solution, yielding micellar association number, hydrodynamic and thermodynamic radius, and the related thermodynamic expansion factor. At higher concentrations, solution of copolymers E<sub>50</sub>S<sub>5.1</sub> and E<sub>51</sub>S<sub>6.5</sub> formed hard isotropic gels.

## 1. Introduction

The association and surface properties of water-soluble block copolyethers based on poly(ethylene oxide) as the hydrophilic and poly(propylene oxide) or poly(butylene oxide) as the hydrophobe attract much attention, not least because they are available from industrial sources: for example, triblock E<sub>m</sub>P<sub>n</sub>E<sub>m</sub> and P<sub>n</sub>E<sub>m</sub>P<sub>n</sub> copolymers from BASF and other sources, triblock E<sub>m</sub>B<sub>n</sub>E<sub>m</sub> and diblock E<sub>m</sub>B<sub>n</sub> copolymers from The Dow Chemical Company. Here E denotes an oxyethylene unit, OCH<sub>2</sub>CH<sub>2</sub>, P an oxypropylene unit, OCH<sub>2</sub>CH(CH<sub>3</sub>), B an oxybutylene unit, OCH<sub>2</sub>CH(CH<sub>2</sub>CH<sub>3</sub>), and subscripts *m* and *n* denote block lengths in chain units. The considerable body of work on aqueous solutions of E<sub>m</sub>P<sub>n</sub>E<sub>m</sub> copolymers has been comprehensively reviewed,<sup>1</sup> and the effect of block architecture in the E/P block copolymer system, including linear and cyclic diblocks, has received attention.<sup>2–5</sup> References concerning work of similar scope on aqueous solutions of E/B copolymers of various architectures can be found in recent publications.<sup>6–9</sup>

Within the family of block copolyethers there are a number of possibilities for preparation of water-soluble block copolymers with highly hydrophobic blocks, one of which is to sequentially copolymerize ethylene oxide and styrene oxide. Compared with the preparation of block copolymers of ethylene oxide and styrene, the preparation of a wholly copolyether makes use of oxyanion chemistry throughout, thus avoiding the less robust carbanion chemistry needed to prepare a polystyrene block.<sup>10</sup>

Previously we have prepared a triblock copolymer, S<sub>4</sub>E<sub>45</sub>S<sub>4</sub>, and studied its association and surface properties in aqueous solution.<sup>11</sup> [Here we use S to denote an oxyphenylethylene unit, OCH<sub>2</sub>CH(C<sub>6</sub>H<sub>5</sub>).] This report concerns an extension of that work, that is, the preparation of three diblock copolymers (E<sub>50</sub>S<sub>3.5</sub>, E<sub>50</sub>S<sub>5.1</sub>, and E<sub>51</sub>S<sub>6.5</sub>) and measurement of their properties in aqueous solution.

## 2. Experimental Section

**2.1. Preparation.** The three diblock copolymers were prepared by sequential anionic polymerization of ethylene oxide (EO) followed by styrene oxide (SO). The monofunctional initiator was 2-(2-methoxyethoxy)ethanol activated by reaction with potassium metal (mole ratio OH/K = 9). An aliquot was transferred to a weighed dried glass ampule that was fitted with a poly-(tetrafluoroethylene) tap and could be attached to and detached from a vacuum line as needed. EO was dried by stirring over CaH<sub>2</sub> (8 h, 0 °C) before being distilled into the reaction ampule under vacuum. After shaking, the ampule was left at room temperature for 1 day, then immersed in a water bath at, successively, 45 °C (2 days) and 65 °C (8 days). Completion of reaction was checked by cooling a part of the ampule and observing the condensation (if any) of unreacted monomer. At this point a small quantity of the homopolymer was removed for characterization.

(10) See, for example, Marti, S.; Nervo, J.; Riess, G. *Prog. Colloid Polym. Sci.* **1975**, *58*, 114; Quirk, R. P.; Kim, J.; Kausch, C.; Chun, M. S. *Polym. Int.* **1996**, *39*, 3.

(11) Mai, S.-M.; Ludhera, S.; Heatley, F.; Attwood, D.; Booth, C. *J. Chem. Soc., Faraday Trans.* **1998**, *94*, 567.

\* Author for correspondence.

<sup>†</sup> University of Manchester.

<sup>‡</sup> National and Kapodistrian University of Athens.

<sup>§</sup> University of Sheffield.

(1) Chu, B.; Zhou, Z.-K. In *Nonionic Surfactants, Polyoxyalkylene Block Copolymers*; Nace, V. M., Ed.; Surfactant Science Series, Vol. 60; Marcel Dekker: New York, 1996.

(2) Zhou, Z.-K.; Chu, B. *Macromolecules* **1994**, *27*, 2025.

(3) Altinok, H.; Yu, G.-E.; Nixon, S. K.; Gorry, S. K.; Attwood, D.; Booth, C. *Langmuir* **1997**, *13*, 5837.

(4) Yu, G.-E.; Garrett, C. A.; Mai, S.-M.; Altinok, H.; Attwood, D.; Price, C.; Booth, C. *Langmuir* **1998**, *14*, 2278.

(5) Altinok, H.; Nixon, S. K.; Gorry, P. A.; Attwood, D.; Booth, C.; Kelarakis, A.; Havredaki, V. *Colloids Surf. B* **1996**, *16*, 73.

(6) Derici, L.; Ledger, S.; Mai, S.-M.; Booth, C.; Hamley, I. W.; Pedersen, J. S. *Phys. Chem. Chem. Phys.* **1999**, *1*, 2773.

(7) Kelarakis, A.; Havredaki, V.; Derici, L.; Yu, G.-E.; Booth, C.; Hamley, I. W. *J. Chem. Soc., Faraday Trans.* **1998**, *94*, 3639.

(8) Yu, G.-E.; Yang, Z.; Attwood, D.; Price, C.; Booth, C. *Macromolecules* **1996**, *29*, 8479.

(9) Liu, T.-B.; Zhou, Z.-K.; Wu, C.-H.; Nace, V. M.; Chu, B. *J. Phys. Chem. B* **1998**, *102*, 2875.

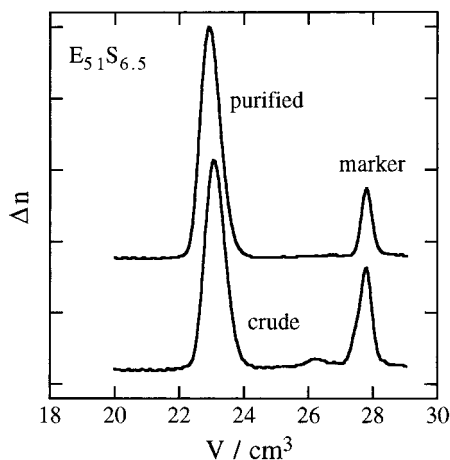


**Figure 1.** GPC curves (refractive index difference,  $\Delta n$ , versus elution volume,  $V$ ) illustrating the purification of copolymer  $E_{51}S_{6.5}$ .

To complete the preparation, SO was stirred overnight with  $\text{CaH}_2$ , and distilled under vacuum onto type 4A mole sieves. The ampule was thoroughly evacuated ( $10^{-4}$  mmHg, 8 h) before purging with dry nitrogen and adding the dry SO via a syringe. After evacuation, the ampule was heated to  $65^\circ\text{C}$  to melt the poly(oxyethylene) and shaken to mix the contents. Polymerization was then allowed to proceed at  $65^\circ\text{C}$  (7 days) and finally  $80^\circ\text{C}$  (21 days). At this stage the copolymer was bright yellow in color, reflecting the presence of  $-\text{CH}(\text{C}_6\text{H}_5)\text{O}^-\text{K}^+$  ion pairs.

Gel permeation chromatography (GPC) was used for initial characterization of the samples: see below for details. The GPC curves of the poly(oxyethylene)s from the first stage of the copolymerizations had single narrow peaks. Those of the crude copolymers had narrow main peaks, but also small peaks at higher elution volume (see Figure 1,  $V \approx 26\text{ cm}^3$ ) that were attributed to homopoly(styrene oxide) resulting from the introduction of moisture (an initiator) at the second stage. The copolymers were purified by fractionation, that is, by precipitating the copolymer from a solution in dichloromethane by addition of hexane. The GPC curves of the purified polymers contained single narrow peaks: see Figure 1.

The yellow coloration persisted throughout the purification procedure, and was eventually removed by dissolving the copolymer in dichloromethane and shaking with dilute HCl in a separating funnel. After washing (distilled water), the organic phase was evaporated and the copolymer dried ( $10^{-4}$  mmHg, 2 days,  $40^\circ\text{C}$ , with stirring).

**2.2. Characterization.** Samples were characterized by GPC and  $^{13}\text{C}$  NMR spectroscopy. The GPC system used consisted of three  $\mu$ -Styragel columns (Waters Associates, nominal porosity from 500 to  $10^4$  Å) eluted by tetrahydrofuran at  $20^\circ\text{C}$ . Samples were injected via a 100 mm $^3$  loop at a concentration of  $2\text{ g dm}^{-3}$ , and their emergence was detected by differential refractometry (Waters Associates model 410). The flow rate was  $1\text{ cm}^3\text{ min}^{-1}$ , monitored by use of an internal marker (dodecane). Calibration was with poly(oxyethylene) samples of known molar mass. Analysis of the GPC curves gave an estimate of width of the molar mass distribution in the form of the ratio of mass-average to number-average molar mass ( $M_w/M_n$ ) as if the samples were poly(oxyethylene).

NMR spectra were recorded by means of a Varian Unity 500 spectrometer operated at 125.5 MHz for  $^{13}\text{C}$  spectra. Solutions were ca. 10 wt % in  $\text{CDCl}_3$ . Assignments were taken from previous work.<sup>12</sup> The integrals of the resonances from backbone and end group carbons were used to determine average composition (i.e., mole fraction  $E$ ) and number-average molar mass. Allowance was made for the different nuclear Overhauser enhancements of E and S units.<sup>12</sup> The NMR spectra of all three copolymers indicated a proportion of E ends terminated with hydroxyl groups, that is, not end-capped by S units. This material was not removed by the purification procedure described above.

Selected molecular characteristics of the precursor poly(oxyethylene)s from the first stage of copolymerization and the final purified samples are listed in Table 1. Values of  $M_w/M_n$  of the homopoly(oxyethylene)s were all 1.02. Also listed are the mole fractions of uncapped poly(oxyethylene) derived from the NMR spectra ( $x_{\text{poe}}$ ), values of  $M_n$  and  $M_w$  for the copolymers corrected for poly(oxyethylene) content, and the mass fraction of uncapped poly(oxyethylene) ( $w_{\text{poe}}$ ). The formulas are for the copolymers, that is, corrected for homopolymer content.

The Weibull–Nycander equation<sup>13,14</sup> can be applied to these results, that is,

$$\frac{k_{\text{SS}}}{k_{\text{ES}}} = \frac{n - 1 + x_{\text{poe}}}{x_{\text{poe}} - \ln(x_{\text{poe}}) - 1} \quad (1)$$

where  $k_{\text{ES}}$  and  $k_{\text{SS}}$  are the rate constants for reaction of SO with an E or an S oxyanion respectively, and  $n$  is the S-block length. Values of  $k_{\text{SS}}/k_{\text{ES}} \approx 2.8 \pm 0.3$  fit the three data points, indicating a relatively slow reaction of SO with an E oxyanion. Under these circumstances the S-block length distribution must be wide. The discernible effects of this on association and surface properties are mentioned in the discussion.

**2.3. Clouding and Gelation.** Clouding and gelation were investigated by visual inspection of 5–70 wt % aqueous solutions of the copolymers. Samples of solution (0.5 g) were enclosed in small tubes (internal diameter ca. 10 mm) and equilibrated at low temperature overnight. The solution was then observed while slowly heating (or cooling) the tube in a water bath within the range  $0$ – $85^\circ\text{C}$ . The heating/cooling rate was  $0.5\text{ deg min}^{-1}$ . The change from a mobile to an immobile system (or vice versa) was determined by inverting the tube. The method served to define the sol–gel transition temperatures to  $\pm 1^\circ\text{C}$ . Previous work has shown that rheometry, calorimetry, and small-angle X-ray scattering all lead to the same hard gel–sol boundaries as the simple tube-inversion method.<sup>15,16</sup>

The gels were examined under crossed polars by means of a Nikon Optiphot microscope equipped with a Mettler hot-stage temperature controller used at a heating rate of  $1\text{ deg min}^{-1}$  over the range  $0$ – $75^\circ\text{C}$ . Evaporation of water was limited by thin coverslips.

**2.4. Surface Tension.** Surface tensions ( $\gamma$ ) of dilute aqueous solutions were measured at four temperatures in the range  $20$ – $50^\circ\text{C}$  by detachment of a platinum ring using a temperature-controlled ( $\pm 0.2^\circ\text{C}$ ) surface tension meter (Kruss, model K8600). The instrument was protected from vibration and drafts. Copolymer solutions in deionized and doubly distilled water were made by dilution of a stock solution. A new solution was first equilibrated at the lowest temperature for 24 h and then  $\gamma$  was measured every 1 h until consistent readings were obtained. Thereafter, the temperature was raised and the procedure repeated. Before a new solution was used, the ring was washed successively with dilute HCl and water. The accuracy of measurement was checked by frequent determination of the surface tension of pure water.

**2.5. Light Scattering.** All glassware was washed with condensing acetone vapor before use. Solutions were clarified by filtering through Millipore Millex filters (Triton free,  $0.22\text{-}\mu\text{m}$  porosity) directly into the cleaned scattering cell.

Static light scattering (SLS) intensities were measured for solutions at temperatures in the range  $20$ – $50^\circ\text{C}$  by means of a Brookhaven BI 200S instrument with vertically polarized incident light of wavelength  $\lambda = 488\text{ nm}$  supplied by an argon ion laser (Coherent Innova 90) operated at 500 mW or less. The intensity scale was calibrated against benzene. Dynamic light scattering (DLS) measurements were made under similar conditions by means of the instrument described above combined with a Brookhaven BI 9000 AT digital correlator. In each case mea-

(13) Weibull, B.; Nycander, B. *Acta Chem. Scand.* **1954**, *8*, 847.

(14) Yu, G.-E.; Yang, Z.; Ameri, M.; Attwood, D.; Collett, J. H.; Price, C.; Booth, C. *J. Phys. Chem.* **1997**, *101*, 4394.

(15) Li, H.; Yu, G.-E.; Price, C.; Booth, C.; Hecht, E.; Hoffmann, H. *Macromolecules* **1997**, *30*, 1347.

(16) Pople, J. A.; Hamley, I. W.; Fairclough, J. P. A.; Ryan, A. J.; Komanschek, B. U.; Gleeson, A. J.; Yu, G.-E.; Booth, C. *Macromolecules* **1997**, *30*, 5721.

(12) Heatley, F.; Yu, G.-E.; Draper, M. D.; Booth, C. *Eur. Polym. J.* **1991**, *27*, 471.

**Table 1. Molecular Characteristics of Samples<sup>a</sup>**

copolymer formula	GPC $M_w/M_n$	NMR					
		$M_n$ E block, g mol <sup>-1</sup>	$M_n$ sample, g mol <sup>-1</sup>	mole fraction $x_{poe}$	mass fraction $w_{poe}$	$M_n$ copolymer, g mol <sup>-1</sup>	$M_w$ copolymer, g mol <sup>-1</sup>
E <sub>50</sub> S <sub>3.5</sub>	1.02	2200	2560	0.15	0.13	2620	2670
E <sub>50</sub> S <sub>5.1</sub>	1.04	2200	2750	0.10	0.08	2810	2920
E <sub>51</sub> S <sub>6.5</sub>	1.03	2240	2980	0.06	0.05	3020	3110

<sup>a</sup> Estimated uncertainties:  $M_w/M_n$ ,  $\pm 0.01$ ;  $M_n$ ,  $M_w$ ,  $\pm 4\%$ .

**Table 2. Specific Refractive Index Increments of Samples<sup>a</sup>**

sample	specific refractive index increment $\nu = dn/dc/cm^3 g^{-1}$	
	20 °C	40 °C
E <sub>50</sub> S <sub>3.5</sub>	0.147	0.144
E <sub>50</sub> S <sub>5.1</sub>	0.153	0.148
E <sub>51</sub> S <sub>6.5</sub>	0.155	0.152

<sup>a</sup> Estimated uncertainty:  $\pm 0.001$ .

measurements of scattered light were normally made at angle  $\theta = 90^\circ$  to the incident beam. Experiment duration was in the range 5–20 min, and each experiment was repeated two or more times.

The correlation functions from DLS were analyzed by the constrained regularized CONTIN method<sup>17</sup> to obtain distributions of decay rates ( $\Gamma$ ). The decay rate distributions gave distributions of apparent diffusion coefficient ( $D_{app} = \Gamma/q^2$ ,  $q = (4\pi n/\lambda)\sin(\theta/2)$ ,  $n$  = refractive index of water) and hence of apparent hydrodynamic radius ( $r_{h,app}$ , radius of the hydrodynamically equivalent hard sphere corresponding to  $D_{app}$ ) via the Stokes–Einstein equation

$$r_{h,app} = kT/(6\pi\eta D_{app}) \quad (2)$$

where  $k$  is the Boltzmann constant and  $\eta$  is the viscosity of water at temperature  $T$ .

The basis for analysis of SLS was the Debye equation

$$K^*c(I - I_s) = 1/M_w + 2A_2c + \dots \quad (3)$$

where  $I$  is intensity of light scattering from solution relative to that from benzene,  $I_s$  is the corresponding quantity for the solvent,  $c$  is the concentration (in g dm<sup>-3</sup>),  $M_w$  is the mass-average molar mass of the solute,  $A_2$  is the second virial coefficient (higher coefficients being neglected), and  $K^*$  is the appropriate optical constant, which includes the specific refractive index increment,  $\nu = dn/dc$ .

Values of  $\nu$  and its temperature increment were determined by means of an Abbé 60/ED precision refractometer (Bellingham and Stanley). Results obtained for the copolymers are listed in Table 2: the temperature dependence, averaging  $2 \times 10^{-4} \text{ cm}^3 \text{ g}^{-1} \text{ K}^{-1}$ , is similar to that found for other block copolyethers.<sup>3,18</sup> A value of  $\nu = 0.169 \text{ cm}^3 \text{ g}^{-1}$  (15 °C) was used for triblock copolymer S<sub>4</sub>E<sub>45</sub>S<sub>4</sub>.<sup>11</sup> Sources of the other quantities necessary for calculating  $K^*$  have been given previously.<sup>19</sup> The effect of the different refractive indices of the blocks on the derived molar mass is considered in Section 3.7.

### 3. Results and Discussion

**3.1. Clouding.** Clouding of aqueous solutions of the copolymers in the concentration range 5–70 wt % were investigated over the temperature range 0–90 °C. All solutions remained clear under these conditions.

**3.2. Confirmation of Micellization.** DLS was used to confirm micellization of the copolymers in dilute aqueous solution.

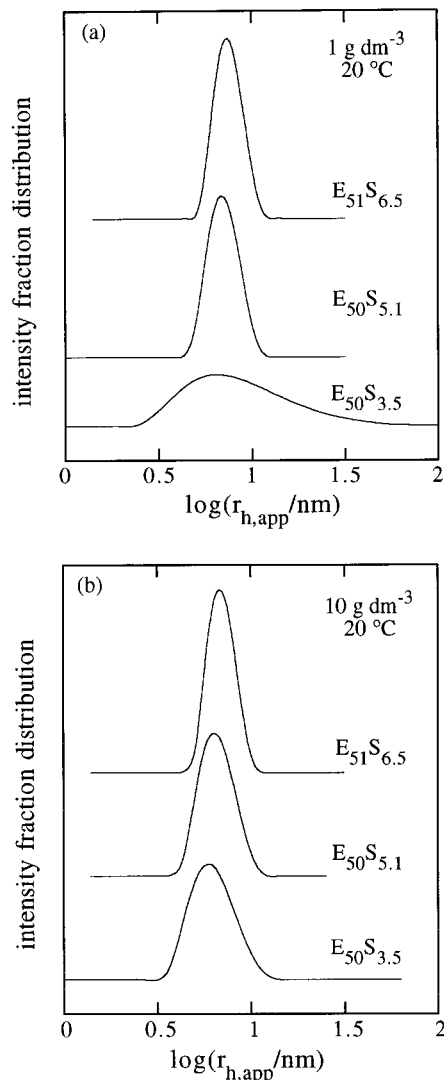


**Figure 2.** Apparent hydrodynamic radius ( $r_{h,app}$ ) from DLS. Intensity fraction distribution  $I(\log r_{h,app})$  versus  $\log(r_{h,app})$  for aqueous solutions at 20 °C of the E<sub>m</sub>S<sub>n</sub> diblock copolymers at concentration: (a) 1 g dm<sup>-3</sup> and (b) 10 g dm<sup>-3</sup>.

Intensity fraction (i.e., normalized) distributions of the logarithm of apparent hydrodynamic radius of micelles in 1 g dm<sup>-3</sup> solution at 20 °C are illustrated in Figure 2a. It is clear that copolymers E<sub>50</sub>S<sub>5.1</sub> and E<sub>51</sub>S<sub>6.5</sub> are well micellized in dilute solution, but that E<sub>50</sub>S<sub>3.5</sub> is not. Increasing the concentration by a factor of five or more led to narrow distributions of apparent micellar radius for all three copolymers: see Figure 2b. The narrow distributions are characteristic of systems undergoing closed association to micelles. The broader distribution found for copolymer E<sub>50</sub>S<sub>3.5</sub> at low concentration is ascribed mainly to the response of the CONTIN analysis to unresolved signals from a significant fraction of unassociated molecules. In agreement with this interpretation, the intensity of light scattered from a 1 g dm<sup>-3</sup> solution

(17) Provencher, S. W. *Makromol. Chem.* **1979**, *180*, 201.

(18) Bedells, A. D.; Arafeh, R. M.; Yang, Z.; Attwood, D.; Heatley, F.; Padgett, J. C.; Price, C.; Booth, C. *J. Chem. Soc., Faraday Trans.* **1993**, *89*, 1235.

(19) Yang, Z.; Yang, Y.-W.; Zhou, Z.-K.; Attwood, D.; Booth, C. *J. Chem. Soc., Faraday Trans.* **1996**, *92*, 257.

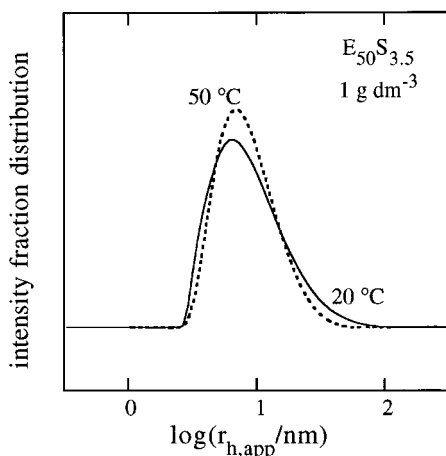


**Figure 3.** Apparent hydrodynamic radius ( $r_{h,app}$ ) from DLS. Intensity fraction distribution  $I(\log r_{h,app})$  versus  $\log(r_{h,app})$  for a  $1 \text{ g dm}^{-3}$  aqueous solution of copolymer  $E_{50}S_{3.5}$  at  $20 \text{ }^\circ\text{C}$  (full line) and  $50 \text{ }^\circ\text{C}$  (broken line).

was found to be some five times lower for copolymer  $E_{50}S_{3.5}$  compared to the other two.

For most block copolyethers the effect of increasing the temperature is to promote micellization. In the case of a poorly micellized copolyether in aqueous solution, increasing the temperature will result in a narrowed intensity fraction distribution. The effect is known to be particularly strong for the  $E_mP_nE_m$  (Pluronic)<sup>1</sup> and related copolymers,<sup>3,5</sup> but it holds for other poly(oxyethylene)-based block copolymers.<sup>6,20</sup> Temperature had a small effect on the distributions of  $\log(r_{h,app})$  of the present copolymers, as illustrated for copolymer  $E_{50}S_{3.5}$  in Figure 3. Insensitivity of association behavior to temperature has been noted previously for certain  $E_mB_n$  copolymers.<sup>7,21</sup> The effect is discussed further in Sections 3.4–3.7.

**3.3. Critical Micelle Concentration.** Plots of surface tension against the logarithm of concentration for aqueous solutions of copolymer  $E_{50}S_{5.1}$  are shown in Figure 4. Similar plots were obtained for solutions of copolymers  $E_{50}S_{3.5}$  and  $E_{51}S_{6.5}$ . As indicated, it was possible to fit each data set with two straight lines, but only with considerable deviation in the region of their intersection. This effect is attributed to the distribution of S-block lengths in the samples (see Section 2.2), including a proportion of uncapped poly(oxyethylene). Following previous practice in our laboratories,<sup>5,17,22</sup> particularly when dealing with a sample deliberately prepared to have a wide block length distribution,<sup>14</sup> and as advocated by others,<sup>23</sup> the critical micelle concentration (cmc) was assigned to the concentration at which the surface tension reached a steady value. Small corrections (13% or less, see Table 1) were made to the cmc to allow for the fact that the poly(oxyethylene) in the samples will not micellize.<sup>24</sup> The values of the cmc so obtained (see Table 3) lay in the range  $0.03 \text{ g dm}^{-3}$  ( $E_{51}S_{6.5}$ ,  $50 \text{ }^\circ\text{C}$ ) to  $0.4 \text{ g dm}^{-3}$  ( $E_{50}S_{3.5}$ ,  $20 \text{ }^\circ\text{C}$ ). These values are consistent with the presence of micelles in  $1 \text{ g dm}^{-3}$  solutions of all the copolymers, as revealed by DLS (see Section 3.2). The relatively high values of the cmc found for copolymer  $E_{50}S_{3.5}$  are consistent with the wider

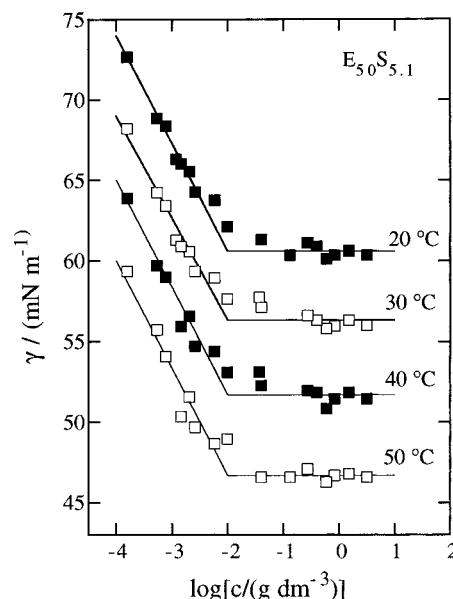


**Figure 4.** Surface tension versus  $\log(\text{concentration})$  for aqueous solutions of copolymer  $E_{50}S_{5.1}$  at the temperatures indicated. For clarity the data are shifted on the ordinate: see Table 3 for actual  $\gamma_{cmc}$  values.

**Table 3. Critical Micelle Concentrations and Surface Tensions for Aqueous Solutions of  $E_mS_n$  Block Copolymers<sup>a</sup>**

copolymer	$T, \text{ }^\circ\text{C}$	cmc, $\text{g dm}^{-3}$	$\gamma_{cmc}, \text{ mN m}^{-1}$
$E_{50}S_{3.5}$	20	0.44	51
	30	0.28	50
	40	0.22	49
	50	0.14	47
$E_{50}S_{5.1}$	20	0.073	52
	30	0.058	50
	40	0.046	49
	50	0.037	47
$E_{51}S_{6.5}$	20	0.048	52
	30	0.044	50
	40	0.038	49
	50	0.030	46

<sup>a</sup> Estimated uncertainties:  $\log(\text{cmc}), \pm 0.1$ ;  $\gamma_{cmc}, \pm 1\%$ .

distributions of apparent hydrodynamic radius found for that copolymer.

Including present results, values of the cmc are now available for three series of diblock polyethers ( $E_mS_n$ ,  $E_mB_n$ , and  $E_mP_n$ ). Adopting the law of mass action to describe the micellization process, and given certain requirements (narrow micelle size distributions and micelle association numbers approaching 50),<sup>21,25</sup> the Gibbs energy of micellization is directly related to the logarithm of the cmc:

$$\Delta_{\text{mic}}G = RT \ln(\text{cmc}) \quad (4)$$

where the cmc is in molar units. Accordingly, recognizing that the micellization process is dominated by the length of the hydrophobic block ( $n$ ), an appropriate basis for comparison of micellization in the three series is a plot of  $\log(\text{cmc})$  against  $n$ : see Figure 5. The data points are for solutions at  $30 \text{ }^\circ\text{C}$ : sources of data for the  $E_mB_n$  and  $E_mP_n$  copolymers are summarized in previous reports.<sup>5,21</sup> If the chain length required to attain a given value of the cmc is used as indicator (i.e., comparison along a horizontal in Figure 5), then the hydrophobicities are seen to be in approximate ratio:

(25) Hall, D. G. In *Nonionic Surfactants, Physical Chemistry*; Schick, M. J., Ed.; Marcel Dekker: New York, 1987; Vol. 23, p 247.

(20) Tanodekaew, S.; Pannu, R.; Heatley, F.; Attwood, D.; Booth, C. *Macromol. Chem. Phys.* **1997**, *198*, 927.

(21) Kellarakis, A.; Havredaki, V.; Yu, G.-E.; Derici, L.; Booth, C. *Macromolecules* **1998**, *31*, 1944.

(22) Yang, Z.; Pickard, S.; Deng, N.-J.; Barlow, R. J.; Attwood, D.; Booth, C. *Macromolecules* **1994**, *27*, 2371.

(23) Alexandridis, P.; Athanassiou, V.; Fukuda, S.; Hatton, T. A. *Langmuir* **1994**, *10*, 2604.

(24) Linse, P. *Macromolecules* **1994**, *27*, 2685.

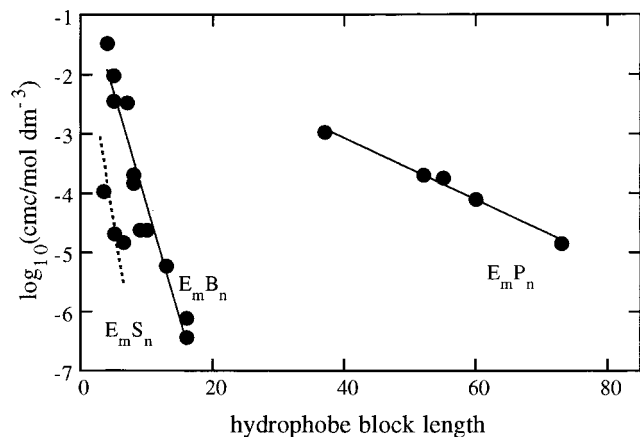


**Figure 5.** Logarithm of cmc (in mol dm<sup>-3</sup>) at 30 °C versus hydrophobe length ( $n$  in S, B, or P units) for  $E_mS_n$ ,  $E_mB_n$ , and  $E_mP_n$  diblock copolymers. The straight lines guide the eye through the points.

$$P:B:S = 1:6:12$$

The ratio of hydrophobicities  $P:S = 1:12$  is the same as that reported earlier.<sup>11</sup>

**3.4. Thermodynamics of Micellization.** A conventional plot of logarithm(cmc) against inverse temperature is shown in Figure 6. Given the requirements described in Section 3.3, that is, a narrow micelle size distribution and a micelle association number approaching 50, and further assuming an association number independent of temperature, the slope of this van't Hoff plot gives the standard enthalpy of micellization,  $\Delta_{mic}H^\circ$ .<sup>21,25</sup> The values obtained from Figure 6 are:

copolymer	$E_{50}S_{3.5}$	$E_{50}S_{5.1}$	$E_{51}S_{6.5}$
$\Delta_{mic}H^\circ/kJ\ mol^{-1}$	29	18	12

In fact the requirements are met for copolymer  $E_{51}S_{6.5}$  but not for copolymers  $E_{50}S_{5.1}$  and  $E_{50}S_{3.5}$ : see Section 3.2 for distributions and Section 3.7 for association numbers. However, whether or not the values of  $\Delta_{mic}H^\circ$  can be applied directly to the equilibrium constant ( $K_{mic}$ ) for the micelle–molecule equilibrium, they do accurately describe the temperature dependence of the cmc. The values of  $\Delta_{mic}H^\circ$  are low compared, for example, to values of 200 kJ mol<sup>-1</sup> or more obtained for  $E_mP_n$  copolymers.<sup>5</sup> They are consistent with the insensitivity to temperature of the micelle size distributions from DLS.

The trend is a decreasing value of  $\Delta_{mic}H^\circ$  as the hydrophobic block length is increased. A similar trend has been found in the standard enthalpies of micellization of  $E_mB_n$  block copolymers,<sup>21</sup> that is, another block polyether system with a highly hydrophobic component. The effect has been ascribed to the hydrophobic blocks being tightly coiled in the dispersed molecular standard state, so that interaction with water is minimized in comparison with shorter blocks, which are relatively extended in the molecular state.<sup>18,21</sup> An unassociated copolymer with one block in a tightly coiled state has been called a monomolecular micelle.<sup>26</sup>

**3.5. Surface Activity.** Considering the surface activity of the copolymers, the minimum values of the surface

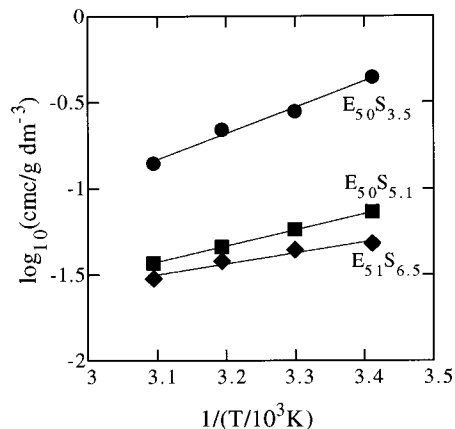


**Figure 6.** Log(cmc) versus reciprocal temperature for aqueous solutions of the  $E_mS_n$  diblock copolymers indicated.

tension beyond the cmc are  $\gamma_{cmc} = 52\text{--}46\text{ mN m}^{-1}$  (see Table 3). Values in this range are typical of block copolyethers with lengthy hydrophobic blocks: for example,  $E_mB_n$ ,  $n \geq 16$ .<sup>21</sup>  $E_mB_n$  copolymers with shorter B blocks,<sup>14,18</sup> and  $E_mP_n$  and  $E_mP_nE_m$  copolymers<sup>5,23,27</sup> show greater surface activity, that is,  $\gamma_{cmc}$  some 10 mN m<sup>-1</sup> lower.

The slope of the  $\gamma\text{--log}(c)$  plot below the cmc can be used to obtain the surface excess concentration through the Gibbs adsorption isotherm,<sup>28</sup> and thereby the area per molecule in the surface monolayer ( $a$ ). As illustrated in Figure 4, the slopes could not be defined with precision in the present work. However, it is noted that the slopes obtained from the straight lines drawn in Figure 4 yield values of  $a$  in the range 0.5–0.9 nm<sup>2</sup>, that is, much as found previously for diblock copolymers of comparable chain length.<sup>18,21</sup>

**3.6. Average Hydrodynamic Radius.** Intensity-average hydrodynamic radii of the micelles of the three copolymers were obtained from DLS. Values were calculated from the intensity-average decay rates output from the CONTIN program. Solutions covering a range of concentrations were investigated at two temperatures, 20 and 40 °C.

Values of the reciprocal apparent hydrodynamic radius obtained for solutions at 20 °C are plotted against concentration in Figure 7. Similar plots were obtained for solutions at 40 °C. Through eq 2,  $1/r_{h,app}$  is proportional to  $D_{app}\eta/T$  and so, compared with  $D_{app}$  itself, is compensated for changes in temperature and solvent viscosity. Extrapolation of the results to zero micelle concentration (essentially equivalent to zero copolymer concentration because the cmc of the copolymers are low; see Section 3.3) gave the values of  $r_h$  listed in Table 4 and (via eq 2) the corresponding values of  $D$ . As described many times previously (see, for example, refs 3–7), a positive slope of a plot of  $1/r_{h,app}$  against concentration, as in Figure 7, is the usual situation for diblock-copolymer micelles.

**3.7. Micelle Molar Mass and Thermodynamic Radius.** The Debye equation (eq 3 of Section 2.5) was the basis of the analysis of SLS from solutions at two temperatures, 20 and 40 °C. The dissymmetry ratio ( $I_{45}/I_{135}$ ) was consistently near to unity for all solutions, that is, the micelle dimensions were small relative to the wavelength of the light, as anticipated considering the values of  $r_h$  measured by DLS.

(26) See, for example, the following reviews. (a) Brown, R. A.; Masters, A. J.; Price, C.; Yuan, X.-F. In *Comprehensive Polymer Science*; Booth, C., Price, C., Eds.; Pergamon Press: Oxford, 1989; Vol. 2, p 185. (b) Tuzar, Z.; Kratochvil, P. In *Surface Colloid Sci.* Vol. 15; Matijevic, E., Ed.; Plenum Press: New York, 1993; p 1. (c) Chu, B. *Langmuir* **1994**, *11*, 414.

(27) Wanka, G.; Hoffmann, H.; Ulbricht, W. *Macromolecules* **1994**, *27*, 4145.

(28) See for example Attwood, D.; Florence, A. T. *Surfactant Systems*; Chapman and Hall: London, 1983; p 14.

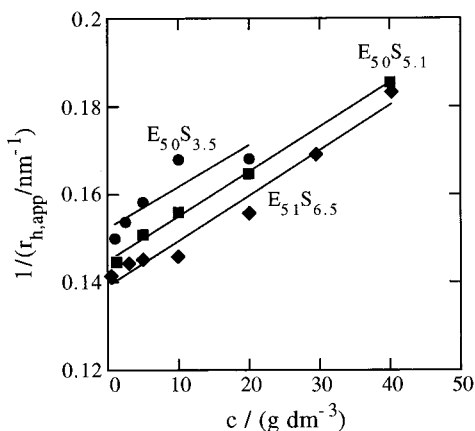


**Figure 7.** Reciprocal of apparent hydrodynamic radius versus copolymer concentration for solutions at 20 °C of the  $E_mS_n$  copolymers. Least-squares straight lines are indicated.

**Table 4. Micellar Properties from Static and Dynamic Light Scattering<sup>a</sup>**

copolymer	$T, ^\circ\text{C}$	static light scattering			dynamic light scattering	
		$M_w, 10^5 \text{ g mol}^{-1}$	$N_w$	$\delta_t$	$D, 10^{-11} \text{ m}^2 \text{ s}^{-1}$	$\eta_h, \text{ nm}$
$E_{50}S_{3.5}$	20	0.50	19	3.7	3.3	6.6
	40	0.65	24	3.1	5.0	7.0
$E_{50}S_{5.1}$	20	1.0	34	4.3	3.1	6.9
	40	1.2	41	3.7	4.8	7.3
$E_{51}S_{6.5}$	20	1.5	48	4.5	3.0	7.2
	40	1.6	51	3.6	4.4	7.8

<sup>a</sup> Estimated uncertainties: all quantities,  $\pm 5\%$ .

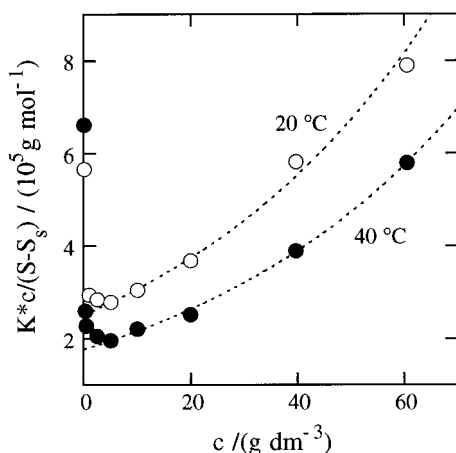


**Figure 8.** SLS. Debye plots for solutions of copolymer  $E_{50}S_{3.5}$  in water at the temperatures indicated.

Use of eq 3 truncated to the second term was not satisfactory, in part because of an increased proportion of unassociated molecules at low concentrations that caused an upturn in the Debye plot, but mainly because of curvature at higher concentrations caused by intermicellar interaction: see Figure 8. Rather than accommodate the curvature by use of a power series (virial expansion), so introducing a number of adjustable coefficients, we have used a method-based scattering theory from hard spheres incorporating the Carnahan–Starling equation.<sup>29,30</sup> This is equivalent to using a virial expansion for the structure factor for hard spheres taken to its seventh term, but requires only two adjustable parameters,  $M_w$  and  $\delta_t$  as

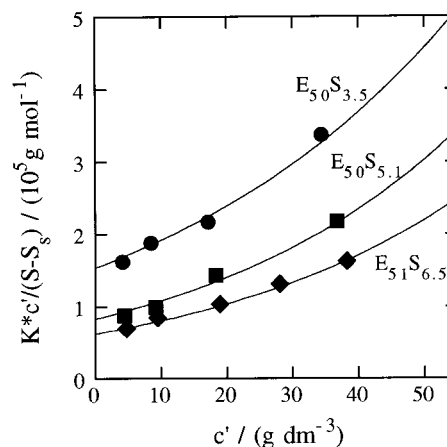


**Figure 9.** SLS. Debye plots (scattering function versus corrected concentration,  $c'$ ) for aqueous solutions of  $E_mS_n$  diblock copolymers at 40 °C. The curves were calculated using eqs 5 and 6.

described below. The new parameter,  $\delta_t$ , relates to the volume excluded by one micelle to another, and it can be applied as an effective parameter for compact micelles irrespective of their exact shape.

In the procedure, the interparticle interference factor (structure factor,  $S$ ) in the scattering equation

$$K^*c/(I - I_0) = 1/SM_w \quad (5)$$

is approximated by

$$1/S = [(1 + 2\phi)^2 - \phi^2(4\phi - \phi^2)](1 - \phi)^{-4} \quad (6)$$

where  $\phi$  is the volume fraction of equivalent uniform spheres. Values of  $\phi$  are calculated from the volume fraction of micelles in the system by applying a thermodynamic expansion factor  $\delta_t$ , that is, the ratio of the thermodynamic volume of a micelle ( $v_t$ ) to its anhydrous volume ( $v_a$ )

$$\delta_t = v_t/v_a \quad (7)$$

where the thermodynamic volume is one-eighth of the volume excluded by one micelle to another. Concentrations were converted to volume fractions assuming densities of dry copolymers in the range  $\rho = 1.12\text{--}1.13 \text{ g cm}^{-3}$ , that is, values are based on liquid densities at 25 °C of  $\rho = 1.12 \text{ g cm}^{-3}$  for poly(ethylene oxide) and  $\rho = 1.15 \text{ g cm}^{-3}$  for poly(styrene oxide).<sup>31,32</sup>

Correction was made for the nonmicellizable poly(oxyethylene) in the samples and for the equilibrium concentration of unassociated copolymer molecules (appreciable only for copolymer  $E_{50}S_{3.5}$ ) by using  $c' = [(1 - w_{\text{poe}})c - \text{cmc}]$  in the analysis (taking  $w_{\text{poe}}$  from Table 1, and cmc from Table 3). To avoid unwanted effects, data points for low concentrations were avoided. Fitting eqs 5 and 6 to the data (see Figure 9 for example) gave the values of  $M_w$  and  $\delta_t$  listed in Table 4. Also listed are mass-average association numbers of the micelles calculated from

$$N_w = M_w(\text{micelle})/M_w(\text{molecule}) \quad (8)$$

using the values of  $M_w(\text{molecule})$  listed in Table 1.

Strictly, the values of  $M_w$  in Table 4 are apparent, and should be denoted  $M_{\text{app}}$ . This is because the specific

(29) Vrij, A. *J. Chem. Phys.* **1978**, *69*, 1742.

(30) Carnahan, N. F.; Starling, K. E. *J. Chem. Phys.* **1969**, *51*, 635.

(31) Mai, S.-M.; Booth, C.; Nace, V. M. *Eur. Polym. J.* **1997**, *33*, 991.

(32) Kern, R. J. *Makromol. Chem.* **1965**, *81*, 261.

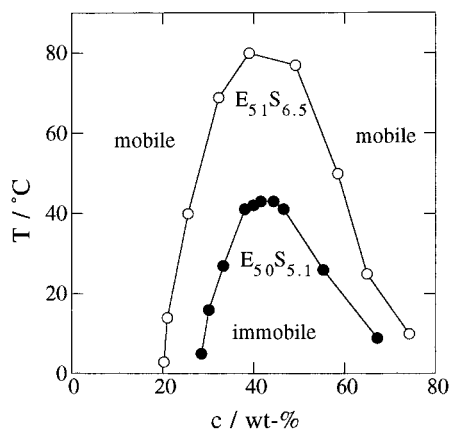


**Figure 10.** Phase (sol-gel) diagram for aqueous solutions of the  $E_mS_n$  diblock copolymers indicated.

refractive index increments of the two pure polymer components differ by  $\Delta\nu \approx 0.1 \text{ cm}^3 \text{ g}^{-1}$ . This means that the ratio  $\Delta\nu/\nu \approx 0.6$ , and this high value must be considered in assessing the validity of  $M_w$ .<sup>33,34</sup> Necessary data are the ratios  $M_w/M_n$  for the two blocks. A value of 1.02 was measured for the E block precursors. Values of 1.2 or less (i.e., the expected values for Poisson distributions)<sup>35</sup> were assumed for the S blocks. Given the mass fractions of E in the copolymer (0.84–0.76), approximate values of the heterogeneity parameters<sup>33</sup> were calculated as  $P/M_w \leq -0.01$  and  $Q/M_w \approx 0.003$ , whence the ratios of the apparent molar mass to the true mass-average molar mass, given by<sup>33</sup>

$$\frac{M_{\text{app}}}{M_w} = 1 + 2 \frac{P \Delta\nu}{M_w \nu} + \frac{Q}{M_w} \left( \frac{\Delta\nu}{\nu} \right)^2 \quad (9)$$

were found to differ by less than 1% from unity. Consequently, the values of  $M_w$  and  $N_w$  listed in Table 4 were accepted without change.

As can be seen in Table 4, the association numbers of the micelles increase by 10–30% in the interval 20–40 °C, whereas those of the hydrodynamic radii increase by 6–8%. As pointed out by Attwood et al., who worked with  $E_mP_nE_m$  copolymers,<sup>36</sup> an increase in temperature will increase the association number but also decrease the swelling of the micelle fringe, both effects being a result of the solvent becoming poorer as temperature is increased. Compensation of these two contributions serves to minimize the effect of temperature on  $\eta_h$ . In the present case it is apparent that the increase in  $N_w$  is marginally the more important.

**3.8. Gelation.** Solutions of the copolymers (5–70 wt %) were investigated for gel formation using the tube-inversion method. The temperature range was 0–90 °C. Solutions of copolymer  $E_{50}S_{3.5}$  did not gel under these conditions, but they did become very viscous at high concentrations (> 60 wt %). Solutions of copolymers  $E_{50}S_{5.1}$  and  $E_{51}S_{6.5}$  formed immobile gels, as shown in Figure 10, that is, gels that were immobile in the inverted tubes over time periods of weeks. Such gels are referred to as hard.<sup>37</sup> Examination by polarized light microscopy showed the

**Table 5. Critical Gel Concentrations and Related Micellar and Molecular Characteristics**

	cgc, g dm <sup>-3</sup> (observed)	cgc, g dm <sup>-3</sup> (calc., fcc)	micelle core radius, nm	S-block length, nm
$E_{50}S_{3.5}$	—	265	1.52	1.27
$E_{50}S_{5.1}$	350	220	2.04	1.82
$E_{51}S_{6.5}$	240	230	2.39	2.17

49 wt %  $E_{51}S_{6.5}$  gel and the 40 wt %  $E_{50}S_{5.1}$  gel to be isotropic, which is a strong indication that they were cubic in structure.

For diblock copolymers in aqueous solution we have shown that the critical gel concentration (cgc) at a given temperature can be predicted from micellar properties measured in dilute solution provided that the structure of the gel is known.<sup>6,38–40</sup> The determining quantities are the thermodynamic expansion factor, related to the excluded volume, and the packing density for the structure, for example

$$\text{cgc}/(\text{g dm}^{-3}) = \frac{740\rho}{\delta_t} \quad (10)$$

for a face-centered cubic (fcc) gel formed from spherical micelles. The first gels formed on increasing the concentration of related  $E_mB_n$  copolymer gels are known to be cubic,<sup>6,16</sup> either body-centered or face-centered according to composition and conditions. A comparison of observed values of the cgc (corrected for the nonmicellizable component and transformed to  $\text{g dm}^{-3}$ ) with values calculated from eq 10 for an fcc gel is shown in Table 5. The relation holds only for the  $E_{51}S_{6.5}$  gel.

A possible explanation of the discrepancy lies in distortion of micelle shape away from sphericity toward cylindrical. Assuming no water penetration of the micelle core, values of core volume, and thereby core radius (see Table 5), for spherical geometry are readily calculated from the molar mass of the S block, the association number, and the anhydrous density of homo(polystyrene oxide). Values of the number-average S-block length can be calculated for a stretched trans-planar conformation assuming an increment of 0.121 nm per chain atom.<sup>41</sup> As seen in Table 5, the spherical core radii are larger than the average block lengths. Because the S blocks must reach the center of the micelle core then, taken at face value, the calculations indicate that spherical micelles cannot form for any of the copolymers.

Alleviation of this severe restriction comes from the distribution of S-block length in the copolymer. Assuming Poisson distributions, the standard deviations of the number distributions of block length, calculated from  $\sigma_n = x_n(x_w/x_n - 1)^{1/2}$ , range from 0.5 ( $E_{50}S_{3.5}$ ) to 0.8 nm ( $E_{51}S_{6.5}$ ). Putting all factors together, the conclusion to be drawn is that the micelles of copolymer  $E_{51}S_{6.5}$  are spherical (or almost so) in their gel phase, but that those of copolymers  $E_{50}S_{3.5}$  and  $E_{50}S_{5.1}$  are elongated; hence eq 10 does not apply. The effect is such that solutions of copolymer  $E_{50}S_{3.5}$  do not form hard gels at any concentration.

**3.9. Comparison with Results for Poly(ethylene oxide)–Poly(styrene) Block Copolymers.** The association properties of diblock copolymers of poly(ethylene oxide) and poly(styrene) have been investigated. However,

(33) Kratochvil, P. *Classical Light Scattering from Polymer Solutions*; Elsevier: Amsterdam, 1987; Chapter 5.

(34) Bushok, W.; Benoit, H. *Can. J. Chem.* **1958**, *36*, 1616.

(35) Flory, P. J. *Principles of Polymer Chemistry*; Cornell University Press: Ithaca, NY, 1953; p. 337.

(36) Attwood, D.; Collett, J. H.; Tait, C. J. *Int. J. Pharm.* **1985**, *26*, 25.

(37) Almgren, M.; Brown, W.; Hvidt, S. *Colloid Polym. Sci.* **1995**, *273*, 2.

(38) Deng, N.-J.; Luo, Y.-Z.; Tanodekaew, S.; Bingham, N.; Attwood, D.; Booth, C. J. *Polym. Sci., Part B: Polym. Phys.* **1995**, *33*, 1085.

(39) Bedells, A. D.; Arafah, R. M.; Yang, Z.; Attwood, D.; Padgett, J. C.; Price, C.; Booth, C. J. *Chem. Soc., Faraday Trans.* **1993**, *89*, 1243.

(40) Yang, Y.-W.; Ali-Adib, Z.; McKeown, N. B.; Ryan, A. J.; Attwood, D.; Booth, C. *Langmuir* **1997**, *13*, 1860.

(41) Flory, P. J. *Statistical Mechanics of Chain Molecules*; Interscience: New York, 1969; p. 165.

rather long block lengths have been used, for example, styrene block lengths up to 108 units by Winnik and co-workers,<sup>42,43</sup> whereas we have restricted attention to shorter hydrophobic blocks. However, work on three copolymers can be usefully compared, that is,  $E_{155}St_{16}$ ,<sup>43</sup>  $E_{68}St_{10}$ ,<sup>44</sup> and  $E_{23}St_8$ ,<sup>45</sup> the last two being commercially available from Goldschmidt AG. Here we use St to denote a phenylethylene unit, retaining S to denote an oxyphenylethylene unit. Reported values of the cmc of two of the copolymers in water are compared with present results in Figure 11. Insofar as can be judged from two small data sets, the micellization properties of the two types of copolymer are similar, no doubt being dominated by the phenyl groups of their hydrophobic blocks. Reported hydrodynamic radii and aggregation numbers are considerably larger than those found in this work for the  $E_mS_n$  copolymers: for example,  $r_h = 10$  nm for  $E_{155}St_{16}$ ,<sup>43</sup>  $r_h = 12-14$  nm and  $N_w > 400$  for  $E_{68}St_{10}$ ,<sup>44</sup> and  $N_w \approx 400$  for  $E_{23}St_8$ .<sup>45</sup>

#### 4. Conclusions

Diblock copolymers of ethylene oxide and styrene oxide ( $E_{50}S_n$ ) with S blocks as short as 3.5 units (on average) micellize efficiently in dilute aqueous solution, association numbers being in the range of 20–50 at 20–40 °C.

(42) Xu, R.-L.; Winnik, M. A.; Hallett, F. R.; Riess, G.; Croucher, M. D. *Macromolecules* **1991**, *24*, 87.

(43) Wilhelm, M.; Zhao, C.-L.; Wang, Y.-C.; Xu, R.-L.; Winnik, M. A.; Mura, J.-L.; Riess, G.; Croucher, M. D. *Macromolecules* **1991**, *24*, 1033.

(44) Mortensen, K.; Brown, W.; Almdal, K.; Alami, E.; Jada, A. *Langmuir* **1997**, *13*, 3635.

(45) Hickl, P.; Ballauff, M.; Jada, A. *Macromolecules* **1996**, *29*, 4006.

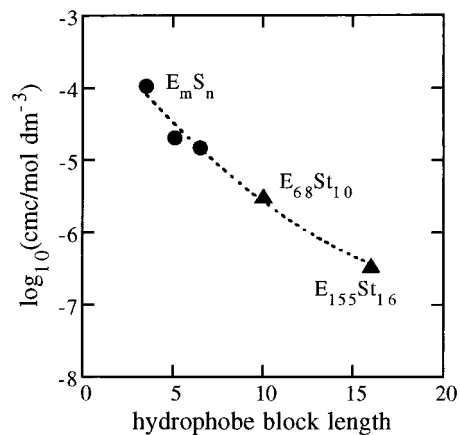


**Figure 11.** Logarithm of cmc (in mol dm<sup>-3</sup>) versus hydrophobe length ( $n$  in S or St units) for  $E_mS_n$  and  $E_mSt_n$  diblock copolymers in aqueous solution at 25–30 °C.

Values of the cmc and  $\Delta_{mic}H^P$  are small, as expected for block copolymers with a highly hydrophobic block. Comparison with the cmc of other block copolyethers, that is,  $E_mP_n$  ( $P$  = oxypropylene) and  $E_mB_n$  ( $B$  = oxybutylene) indicates hydrophobicities in ratio P:B:S = 1:6:12.

Micellar solutions of copolymers  $E_{50}S_{5.1}$  and  $E_{51}S_{6.5}$  formed gels at high concentrations. Micellar solutions of copolymer  $E_{50}S_{3.5}$  formed only a viscous phase.

LA991004O